UHASSELT
KNOWLEDGE IN ACTION

Maastricht University

Faculty of Medicine and Life Sciences
School for Life Sciences
Master of Biomedical Sciences

Master's thesis

Fungal traces in soil: the guild-specific decomposition of mycorrhizal fungal necromass

Birk Auwerkerken

Thesis presented in fulfillment of the requirements for the degree of Master of Biomedical Sciences, specialization Environmental Health Sciences

SUPERVISOR :

Prof. dr. Nadejda SOUDZILOVSKAIA

MENTOR :

De heer Olivier NOUWEN

2024
2025

Transnational University Limburg is a unique collaboration of two universities in two countries: the University of Hasselt and Maastricht University.

UHASSELT
KNOWLEDGE IN ACTION

www.uhasselt.be
Universiteit Hasselt
Campus Hasselt:
Martelarenlaan 42 | 3500 Hasselt
Campus Diepenbeek:
Agoralaan Gebouw D | 3590 Diepenbeek

Faculty of Medicine and Life Sciences
School for Life Sciences
Master of Biomedical Sciences

Master's thesis

Fungal traces in soil: the guild-specific decomposition of mycorrhizal fungal necromass

Birk Auwerkerken

Thesis presented in fulfillment of the requirements for the degree of Master of Biomedical Sciences, specialization Environmental Health Sciences

SUPERVISOR :

Prof. dr. Nadejda SOUDZILOVSKAIA

MENTOR :

De heer Olivier NOUWEN

Fungal traces in soil: the guild-specific decomposition of mycorrhizal fungal necromass*

Birk Auwerkerken[1], Olivier Nouwen[1,2,3], and Nadia Soudzilovskaia[1]

1. Centre for Environmental Sciences, Universiteit Hasselt, Campus Diepenbeek, Agoralaan Gebouw D - B-3590 Diepenbeek
2. Institute of Biology, Leipzig University, Puschstr. 4, 04103 Leipzig, Germany.
3. German Centre for Integrative Biodiversity Research (iDiv) Halle-Jena-Leipzig, Puschstr. 4, 04103 Leipzig, Germany.

**Mycorrhizal fungal necromass decomposition (< 50 characters inc. spaces, italic)*

Correspondence:
Prof. Dr; Nadia Soudzilovskaia, Tel: +3211268262; Email: Nadia.Soudzilovskaia @uhasselt.be

Keywords: Carbon cycle, mycorrhizal fungi, climate change, decomposition, necromass

---

ABSTRACT

Mycorrhizal fungi mediate carbon and nutrient cycling in terrestrial ecosystems, substantially influencing the formation of soil organic carbon (SOC). Despite their recognized role, the specific contributions of arbuscular (AMF), ectomycorrhizal (ECMF), and ericoid mycorrhizal fungi (ERMF) to SOC formation and stabilization remain poorly understood. Here, we present a controlled greenhouse pot experiment directly comparing the decomposition dynamics of these three major mycorrhizal guilds. We quantified decomposition rates across five weeks and examined fungal biochemical traits previously associated with decomposition, including melanin content and hydrophobicity. We hypothesized that these characteristics would be guild-dependent due to similar evolutionary history and functional traits within each guild, therefore showing similar decomposition profiles for each guild. Arbuscular mycorrhizal fungal biomass exhibited significantly slower decomposition than ECMF and ERMF biomass. Interspecific variation in decomposition rate was highest among ECMF and ERMF, which was also observed for melanin and hydrophobicity. We found that melanin and hydrophobicity were not consistent predictors of decomposition rates. These results not only expand fundamental knowledge of fungal necromass turnover but also carry broader implications for modelling soil carbon dynamics in terrestrial ecosystems. By integrating more information on AMF decomposition, we can improve predictions of mycorrhizal contributions to long-term carbon storage, which is critical in the current climate context.

INTRODUCTION

Soil harbors more carbon (C) than the atmosphere and all of Earth's vegetation combined, making it one of the planet's largest C reservoirs (1). In general, ecosystem C accumulation is driven by plants, which capture atmospheric carbon dioxide and convert it into C-rich compounds through photosynthesis. A fraction of this C is immediately released into the atmosphere through respiration, while the remainder is used for plant biomass production, with up to 13% being 'fed' to plant-associated microorganisms (2). Carbon stored in plant biomass is subsequently consumed by fauna and broken down by soil invertebrates and microorganisms, with decomposition rates ranging from days to decades, depending on environmental factors (3). Particularly, plant litter input quality and microbial activity are critical determinants regulating the decomposition rate of organic matter (4). Litter quality characteristics such as high nitrogen (N) levels, high phosphorus (P) levels, low lignin concentrations, and a low C:N ratio promote faster decomposition (5). Furthermore, higher temperatures and moisture levels also accelerate decomposition, facilitating faster C cycling in terrestrial ecosystems (6). While decomposition releases carbon dioxide back into the atmosphere, some organic constituents are harder to break down (e.g., lignin) and are selectively preserved in the soil, forming precursors to stable soil organic matter. In this way, C in the form of soil organic matter can be stored in the soil for thousands of years, preventing it from influencing the climate (7); knowledge about the fluctuation of soil C levels and their return to the atmosphere through decomposition is essential for global climate change predictions (8).

Fungi, as primary decomposers of plant litter and soil organic matter, mediate C and nutrient cycles in terrestrial ecosystems. Moreover, approximately 50,000 fungal species, known as mycorrhizal fungi, form mutualistic relationships with plants by connecting to their roots through an extensive underground network of hyphae (9). There are three main types of mycorrhiza-plant associations, varying in functionality and morphology: arbuscular mycorrhizal fungi (AMF) and ericoid mycorrhizal fungi (ERMF), which penetrate plant root hair cells, and ectomycorrhizal fungi (ECMF), which surround root hair cells without penetrating them (10). Through their underground network, mycorrhizal fungi scavenge for essential resources such as N, P, sulfur (S), trace elements, and water in exchange for photosynthetically derived C from their plant partners (10, 11). However, because of their different evolutionary backgrounds, nutrients may be scavenged through distinct pathways depending on the mycorrhizal association. Arbuscular mycorrhizal fungi dominate in relatively nutrient-rich grasslands and forests and rely on the uptake of inorganic N and P because they lack the enzymes necessary to mineralize organic compounds (12, 13). In contrast, ECMF and ERMF generally prevail in northern temperate forests and heathlands, respectively, using an array of oxidative enzymes to access both organic and inorganic nutrient forms (14, 15). Mycorrhizal fungi thus provide an essential part of plant nutrition; depending on the mycorrhiza-plant relation, up to 80% of P (16) and up to 20% of N (17) are provided through mycorrhizal pathways. Via this nutrient exchange, plants with mycorrhizas, which include over 85% of vascular plants across vegetated terrestrial biomes, serve as a direct C-flux from the atmosphere into the soil, making them an essential player in the carbon cycle (12). Consequently, 36% of current annual CO_2 emissions from fossil fuels are estimated to be fixed by terrestrial plants and allocated to the underground mycelium of mycorrhizal fungi (2). However, mycorrhizal networks exhibit rapid turnover and replacement, up to 60 times per year for arbuscular mycorrhizal fungi (AMF) (18) and up to 20 times per year for ectomycorrhizal fungi (ECMF) (19), depositing substantial amounts of C and nutrients in the soil as dead fungal biomass, also known as necromass. The contribution of different mycorrhizal fungi to the size and stability of the soil carbon pool can vary depending on their biochemical characteristics, and may be influenced by functional traits such as spore production, nutrient acquisition, or the extent of extracellular root colonization (20-23). This raises important questions about the decomposition of microbial necromass and the contributions of different mycorrhizal species to soil C storage. In particular, knowledge about the decomposition of AMF is missing, despite them being associated with 72% of vascular plants (14).

Previous research has identified two factors that may influence the decomposition of fungal

necromass. Firstly, their elemental and structural composition, which differ distinctly between mycorrhizal guilds, has been shown to affect decomposition rates (24, 25). In particular, variations in cell wall composition play a key role, as the cytoplasmic fraction of fungal cells is highly labile and rapidly assimilated by decomposers (26). One key cell wall component is a group of dark brown pigment molecules collectively called melanins which provide protection against environmental stressors such as UV radiation (27), water availability (28), and heavy metals (29). Due to their complex and irregular structure of aromatic monomers, melanins require oxidative enzymes to be broken down and can significantly slow down the decomposition of mycorrhizal necromass (30). Furthermore, melanin might slow down the decomposition of mycorrhizal necromass through the inhibition of extracellular enzymes responsible for the decomposition of cell wall components, with chitinase activity being specifically halted by increased melanin presence (31, 32). In fact, melanins have been identified as the dominant polymers remaining after long-term decomposition experiments, suggesting that they play a major role in the long-term incorporation of carbon from mycorrhizal fungi into soil organic matter pools (30, 33). Additionally, C=C and C=N bonds in aromatic compounds, which are positively correlated with melanin content, have been shown to persist after microbial degradation of mycorrhizal necromass, thereby slowing its decomposition (30). However, it is unknown whether melanin is the most determining molecule during decomposition or whether other molecules incorporated in fungal biomass induce the same effect. Furthermore, there might be a difference in the melanin content and the general chemical composition of different fungal structures. Spores, which are specifically produced to be resistant against environmental stressors, might make up a significant portion of the recalcitrant necromass fraction after bacterial decomposition (34). While it is believed that chemical differences are either manifested in a phylogenetic manner or are likely due to differences in functionality between fungal species, the link between the chemical composition of different mycorrhizal fungi during decomposition remains unclear.

Secondly, the hydrophobicity of fungal necromass may influence decomposition rates, as more hydrophilic compounds are more readily transported into the intracellular space by microorganisms (35). In contrast, more hydrophobic compounds have been reported to prevent the access of degrading enzymes and microorganisms (36). Furthermore, hydrophobic mycelium might clump together in a more hydrophilic environment, forming decomposition-resistant mycelium aggregates (37, 38). Nonetheless, while increased hydrophobicity of soil organic matter has been suggested to slow degradation by decomposers, this property has not yet been properly researched across mycorrhizal fungal guilds (39).

Despite what is known about the role of mycorrhizal fungi in carbon cycling, significant knowledge gaps persist in understanding how decomposition varies among different mycorrhizal guilds, which may indicate distinct contributions to the carbon cycle. Specifically, a comparison between the different fungal characteristics that influence the decomposition process could determine the roles of the different mycorrhizal guilds in relation to soil carbon storage. The goal of this study was to investigate how necromass chemistry and hydrophobicity are related to the decomposition rates of ERMF, ECMF, and AMF. Specifically, we asked ourselves the following questions:

I.) How do decomposition rates vary across the different mycorrhizal guilds?
II.) How are necromass chemistry and hydrophobicity related to the different mycorrhizal guilds?
III.) How are necromass chemistry and hydrophobicity related to mycorrhizal decomposition rates?

Because of their different evolutionary history and functional traits, we hypothesized that mycorrhizal decomposition would decrease in a guild-dependent manner due to varying necromass hydrophobicity and melanin content. In order to investigate this, four mycorrhizal species of the three different guilds were decomposed for up to five weeks in a controlled greenhouse pot experiment using mesh bags. Prior to decomposition, we assessed the differences in mycelial hydrophobicity and necromass chemistry.

EXPERIMENTAL PROCEDURES

Biomass generation

Malt extract agar (MEA) (40) and Czapek Dox Agar (CDA) (41) in mono-compartment plates (Sarstedt) were used to culture the ECMF and ERMF, respectively. Ectomycorrhizal fungi were isolated and obtained from National Park Hoge Kempen and INRAE, while ERMF species were sourced from the University of Turin. Autoclaved cellophane sheets (Colacel) were overlaid on both growth media to facilitate the separation of the mycelium from the agar surface after growth. Additionally, transformed carrot roots and AMF spores were sourced from the *in vitro* collection, GINCO, Belgium, and cultured according to the methods of the Laboratory of Mycology of UCLouvain. Strullu Romand Modified medium (SRM) (42) in bicompartment root organ Petri dish cultures (Greiner bio-one) was used to culture the AMF (24).

Medium containing AMF mycelium and spores were excised from bi-compartment plates and dissolved in a citric acid buffer for several hours to ensure complete dissolution. The fungal biomass was subsequently washed three times in a 10 nM magnesium sulphate ($MgSO_4$) solution. For ECMF and ERMF cultures, mycelium was carefully scraped from the surface of the cellophane sheets and subjected to the same series of washing steps with citric acid buffer and $MgSO_4$ to minimize any residual treatment effects. Following washing, the fungal biomass was flash-frozen in liquid nitrogen and lyophilized overnight (VirTis) to obtain dried fungal biomass pellets. Either dried pellets or fresh mycelium on plates were used to obtain information about the biochemical characteristics of the different mycorrhizal species.

Fungal hydrophobicity measurement

The hydrophobicity of the different mycorrhizal species of ECMF and ERMF was measured using the alcohol percentage test described by Chau et al. (43). Due to the culturing conditions needed for AMF, we were unable to assess their hydrophobicity. A series of ethanol-water dilutions, increasing in 5% ethanol increments, was prepared. Ethanol droplets (8 µl) were deposited onto the mycelium, and the dilution at which the droplet was absorbed into the mycelium within 5 seconds was recorded. Droplets of a higher dilution vanishing indicated increased surface hydrophobicity.

Fungal melanin content measurement

A melanin extraction was performed as described by Lenaers *et al*. to study the melanin content of mycorrhizal necromass (44). Dried fungal pellets were transferred to 15 ml Falcon tubes containing five ml of absolute ethanol and stored in a heating block at 60 °C for 3 hours. After the heating period, the samples were vortexed and centrifuged for 10 min at 4000 revolutions per minute (rpm). The supernatant was removed, and the pellets were kept in the lyophilizer overnight. Then, 1 ml of distilled water was added to each of the samples and gently vortexed. The solution was transferred to glass tubes, after which the samples were resuspended in 1 ml of 6 M HNO_3. The glass tubes were stored in a heating block for three hours at 75 °C. Then, 5 ml of distilled water was added, and the samples were gently vortexed. The solution was transferred to 15 ml Falcon tubes and centrifuged for 10 min at 4000 rpm. The supernatant was removed, and the pellet was transferred to a glass tube with 1 ml of distilled water. Five millilitres of 0.5 M NaOH was added to the glass tubes, and the suspension was kept in heating blocks at 75 °C for 20 min. The suspension was filtered with grade 1 Whatman filter paper (Sigma). One millilitre of the filtered suspension was transferred to a cuvette. Absorbance was measured with a spectrophotometer at 470 nm and compared with a standard curve for synthetic melanin (Sigma). The standard curve was generated from a 1:2 dilution series from 75 mg/l synthetic melanin dissolved in 0.5 M NaOH to 0 mg/l.

Decomposition experiment setup

Dried fungal biomass pellets were put into 15 µm mesh bags of 6 by 6 cm (Teknik filtrations) to be used during the decomposition experiment. The mesh size was chosen to prevent plant roots from infiltrating the sample material. In this way, sample contamination due to the mixing of the roots with the mycorrhizal necromass was avoided. Due to the differences in growth and culturability, initial fungal necromass differed between species. The initial necromass for each mycorrhizal species can be found in Table S1.

To avoid species-specific decomposition traits, each mycorrhizal guild was represented by four species. Furthermore, five biological repeats per

mycorrhizal species were used for each of the ECM (i.e., *Amanita rubescens*, *Hebeloma mesophaeum*, *Laccaria bicolor, Thelephora terrestris*) and ERM (i.e., *Hymenoscyphus ericae*, *Oidiodendron maius* from an unpolluted site = 4, *Oidiodendron maius* from a cadmium-polluted site = 2, and *Hyaloscypha bicolor* = 8) species to ensure statistical power. Due to the difficult culturability of AMF, one repeat was used for *Rhizophagus irregularis* (41833), *Rhizophagus intraradices,* and *Glomus hoi*. Moreover, two repeats were used for *Rhizophagus irregularis* (43194), and three repeats were used for *Rhizophagus aggregatus.* To provide a separate decomposition environment, i.e., one pot for each species, 48 pots (three guilds x four species x one to five biological repetitions) were used.

Each 15 x 40 x 40 cm pot was filled up to 20 cm with a mixture of industrial sand and heathland sod (originating from a heather stand with a dry sandy soil) and a five-centimetre top layer of heathland sod to mimic the mycotron heathland experiment (45). To ensure an identical soil microbiome across all pots, both the heathland sod and sand were autoclaved. Each pot was provided with four non-mycorrhizal *J. effusus* plants to create a more realistic soil environment. Additionally, a microbial inoculum from a soil sample (gathered from the mycotron field experiment) was extracted by mixing 40 grams of soil with 2 l of water by oscillation at 200 rpm for 30 minutes (46, 47). The pots were kept at controlled greenhouse conditions with an air temperature of 23°C, soil moisture of around 50%, and a pH ranging from 4,73 to 6,61 with an average of 5,80 across all pots. At the centre of each pot, three necromass samples were buried at a depth of 10 cm. In this way, the samples were decomposed in identical environments at the soil depth of peak mycorrhizal occurrence (48). Separate samples for each sample time point were stored in individual mesh bags to ensure easy retrieval. Each pot contained one mesh bag sample for every time point of only one mycorrhizal fungal species to avoid decomposition interactions between mycorrhizal species. Furthermore, the individual mesh bags containing the fungal samples were dunked into water right before burial in order to avoid the hydrophobic effects that can be induced by the small mesh size of the mesh bags (49). The mesh bags were retrieved at one, two, three, and four (only for AMF) weeks post-burial, allowing for analysis at nearly complete decomposition, as well as at intermediary time points. Mesh bags were lyophilized upon retrieval.

Chemical spectrum comparison

Next, the chemical fingerprints of undecomposed fungal necromass from all species were analysed using attenuated total reflectance Fourier-transform infrared (ATR-FTIR) spectroscopy (PerkinElmer, Frontier) to explore potential relationships between initial necromass chemistry and mycorrhizal decomposition. Single-point measurements were recorded for each dried fungal pellet, and spectral data were processed for comparative analysis. Localized peak height values were used to compare the absorption intensities of the different fungal species.

Spore extraction and enumeration

To determine spore abundance between different AMF throughout decomposition, spores were extracted from necromass samples at each time point according to Boyno et. al. A fraction of up to 1mg of AMF necromass was mixed with 15 ml of distilled water using a magnetic stirrer at 4–5 rpm for 5 minutes. The mixture was then manually separated and sonicated for 37 kHz for 30 seconds using an ultrasonic cleaner (Elmasonic select). After sonication, the suspension was transferred to a 2 ml Eppendorf tube and further separated using a Retsch Mixer Mill 400 at 20 rpm for 10 minutes. Spores were quantified in 1 ml of supernatant, using a Nikon SMZ 800 bino and ImageJ.

Statistics

After assessing normality and homoscedasticity, a one-way ANOVA followed by a Tukey post-hoc test was used to analyse the differences in necromass loss, surface hydrophobicity, melanin content, and localized peak height in the FTIR spectra. This approach allowed for the comparison of each mycorrhizal guild and between different mycorrhizal fungal species. If assumptions were not met, a Kruskal-Wallis test was performed, followed by a Wilcoxon rank-sum test. Principal component analysis was used to visualize the differences in FTIR topography.

RESULTS

1. Mycorrhizal decomposition rates

Necromass loss differed significantly among mycorrhizal fungal guilds, with the greatest initial loss observed for ECMF and ERMF, respectively (Fig. 1). One week post-burial, ERMF exhibited less mass loss relative to ECMF; however, this difference decreased by week two and was no longer present at week three. In contrast, AMF consistently exhibited significantly lower necromass loss throughout the entire decomposition experiment compared to both ERMF and ECMF. Subsequently, AMF were subjected to decomposition for a longer period. At week five, over 50% of the original AMF necromass remained (Fig. S1), while by week three ECMF and ERMF necromass decreased to ±20% and ±25%, respectively (Fig. 1).

Species within the same guild showed differences in decomposition patterns (Figure 2). Due to the limited number of replicates caused by the challenging culturing conditions of AMF, only one AMF species, i.e., MUCL 49408 (Rhizophagus aggregatus), was included in the statistical comparisons. Consistent with the guild-level patterns, all AMF species displayed lower necromass loss compared to ERMF and ECMF species, with *R. aggregatus* showing the least necromass loss of all species examined (Fig. 2). Following *R. aggregatus*, *H. ericae*, and *T. terrestris* exhibited the lowest necromass loss, with *H. bicolor* following closely behind. By week two, the necromass loss among these three species converged, and they remained the most recalcitrant after *R. aggregatus*. *L. bicolor* and *O. maius* (4) showed intermediate levels of mass loss relative to the other included species, with *L. bicolor* remaining more recalcitrant than *O. maius* (4). In contrast, *O. maius* (2) initially showed comparable mass loss to *L. bicolor yet* lost the second most mass together with *H. mesophaeum*. Furthermore, *A. rubescens* and *H. mesophaeum* were the least recalcitrant during the entire experiment.

2. Biochemical characteristics of mycorrhizal fungi

2.1 Melanin content

Melanin content varied significantly among several mycorrhizal species across and within guilds, despite the differences not being uniform across all pairwise comparisons (Fig. 3). However, *H. ericae* and *O. maius* (4) consistently exhibited significantly higher and intermediate melanin levels, respectively, relative to the other species. In the same way, *G. hoi*, *R. intraradices*, and *L. bicolor* showed distinctly lower melanin levels. Notably, melanin content differed between species of the same guild, suggesting that melanin levels were not guild-dependent in the culturing conditions used during this experiment.

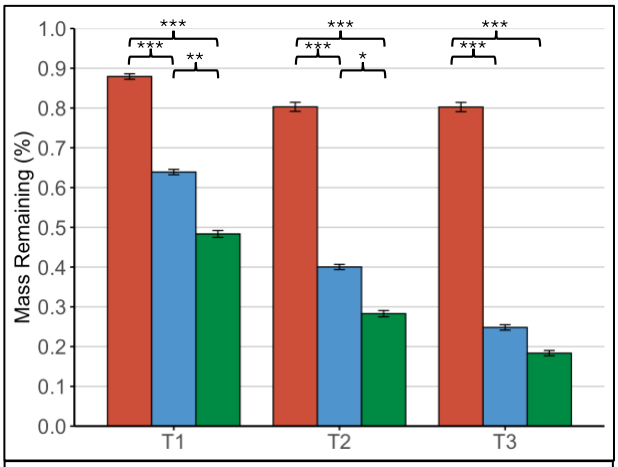

Fig. 1: Average relative mass remaining (± SE) of five AMF (brown), four ERMF (blue), and four ECMF (green) species at one (T1), two (T2), and three (T3) weeks post-decomposition using a controlled pot decomposition experiment. Mass remaining is specified as the percentage of dry weight remaining compared to the original undecomposed necromass sample. Differences in necromass loss across fungal guilds are signified with different asterisks as indicated by a Wilcoxon rank sum test ($p < 0,05$ = *, $0,001 < p < 0,01$ = **, $p < 0,001$ = ***). MUCL 45686 = *Glomus hoi* (n=1), MUCL 41833 = *Rhizophagus irregularis* (n=1), MUCL 49413 = *Rhizophagus intraradices* (n=1), MUCL 49408 = *Rhizophagus aggregatus* (n=3), MUCL 43194 = *Rhizophagus irregularis* (n=1), 2 = *Oidiodendron maius* (n=5), 4 = *Oidiodendron maius* (n=5), He = *Hymenoscyphus ericae* (n=5), 8 = *Hyaloscypha bicolor* (n=5), Hm = *Hebeloma mesophaeum* (n=5), Ar = *Amanita rubescens* (n=5), Tt= *Thelephora terrestris* (n=5), Lb = *Laccaria bicolor* (n=5).

2.6 Hydrophobicity

In general, hydrophobicity levels of ERMF were higher than ECMF, with guild averages of 44% and ±28% ethanol absorption, respectively. However, similar to melanin content, hydrophobicity levels differed significantly between species of the same guild (Fig. 4). *O. maius* (2), *O. maius* (4), and *H. mesophaeum* exhibited the highest surface hydrophobicity of all mycorrhizal species

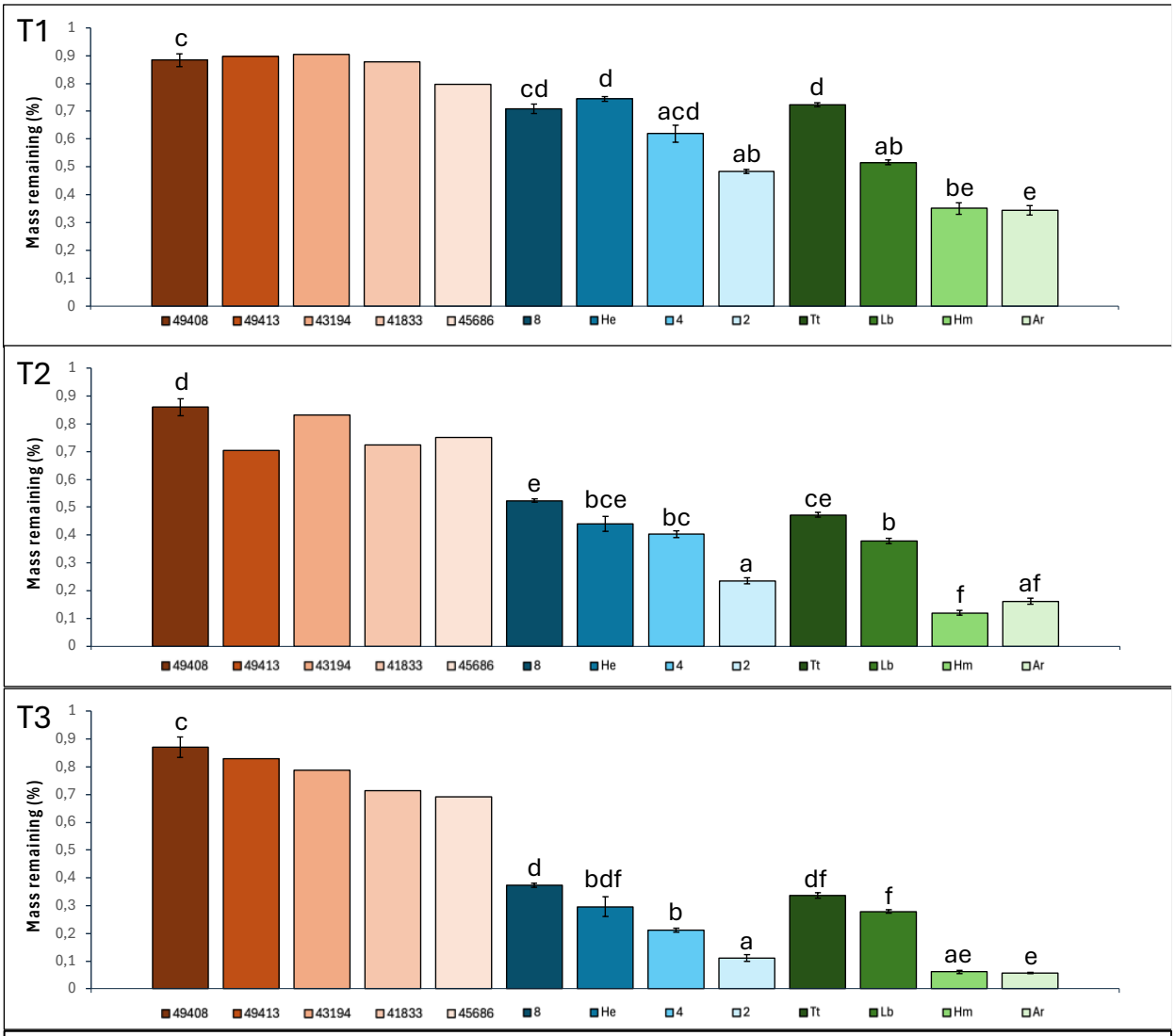

Fig. 2: Relative mass remaining (± SE) of five AMF (brown), four ERMF (blue), and four ECMF (green) species at one (T1), two (T2), and three (T3) weeks post-decomposition using a controlled pot decomposition experiment. Mass remaining is specified as the fraction of dry weight remaining compared to the original undecomposed necromass sample. A Kruskal-Wallis test ($p < 0.05$) showed significant differences in the amount of mass remaining among species. Differences in relative mass remaining across fungal species are signified with different letters as indicated by a Wilcoxon rank sum test ($p<0,05$). Difficult culturing conditions provided enough necromass for only one arbuscular mycorrhizal species (MUCL 49408) to be included in statistics. MUCL 45686 = *Glomus hoi* (n=1), MUCL 41833 = *Rhizophagus irregularis* (n=1), MUCL 49413 = *Rhizophagus intraradices* (n=1), MUCL 49408 = *Rhizophagus aggregatus* (n=3), MUCL 43194 = *Rhizophagus irregularis* (n=1), 2 = *Oidiodendron maius* – polluted origin (n=5), 4 = *Oidiodendron maius* – unpolluted origin (n=5), He = *Hymenoscyphus ericae* (n=5), 8 = *Hyaloscypha bicolor* (n=5), Hm = *Hebeloma mesophaeum* (n=5), Ar = *Amanita rubescens* (n=5), Tt= *Thelephora terrestris* (n=5), Lb = *Laccaria bicolor* (n=5).

examined. Next, *A. rubescens* was slightly more hydrophilic but was still relatively hydrophobic compared to the other mycorrhizal species. Furthermore, *H. bicolor* (8) and *H. ericae* showed intermediate hydrophobicity levels. Notably, *T. terrestris* and *L. bicolor* were the most hydrophilic, with *L. bicolor* absorbing 0% ethanol (=100% milli-Q) droplets. Due to the nature of the alcohol percentage test and the specific culturing conditions required for AMF (42), these species could not be included in hydrophobicity testing.

2.5 *Spore count*

To assess their potential role in the recalcitrance of AMF biomass, spores were quantified per mg of dry weight at one and five weeks post-decomposition. If spores were more recalcitrant than hyphae, the number of spores per mg of necromass was expected to be higher at week five than at week one. However, only *Rhizophagus irregularis* (MUCL 41833) showed a substantial increase in spores per mg of necromass (Fig. 5). The other species showed only slight increases (i.e., *R. irregularis* MUCL 43194 and *R. intraradices)* or slight decreases (i.e., *G. hoi* and *R. aggregatus*).

2.4 FTIR spectroscopy

In general, FTIR absorption spectra of AMF and ERMF were more similar to each other than to the spectrum of ECMF (Fig. 7). These similarities were the most pronounced at wavenumbers of aromatic C-H, aliphatic C-H, and aldehydes/ketones C=O, where AMF and ERMF consistently showed more pronounced peaks than ECMF (Fig. 6).

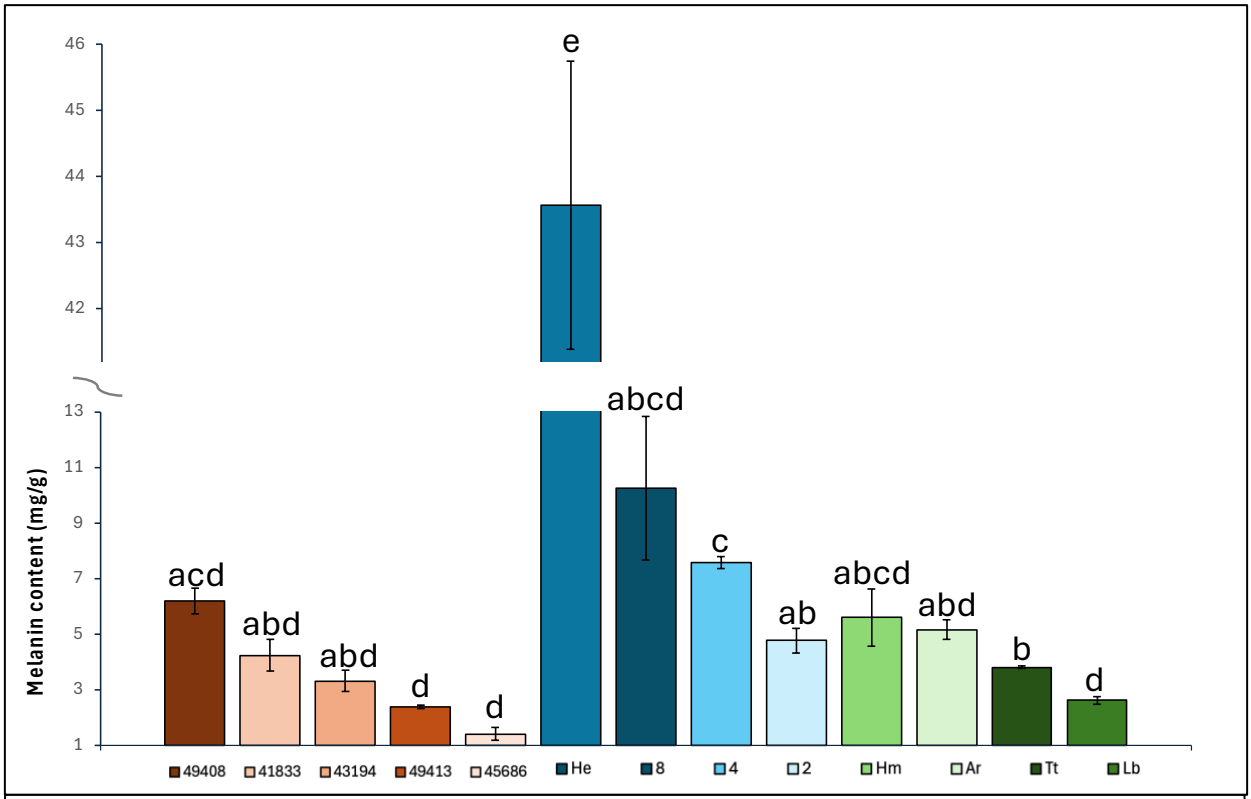

Fig. 3: Necromass melanin content of five AMF (brown), four ERMF (blue), and four ECMF (green) species. Melanin content is specified as mg per gram dry weight necromass ± SE based on three replicates. Differences in melanin content across fungal species are signified with different letters as indicated by a Wilcoxon rank sum test ($p<0,05$). MUCL 45686 = *Glomus hoi*, MUCL 41833 = *Rhizophagus irregularis*, MUCL 49413 = *Rhizophagus intraradices*, MUCL 49408 = *Rhizophagus aggregatus*, MUCL 43194 = *Rhizophagus irregularis,* 2 = *Oidiodendron maius*, 4 = *Oidiodendron maius*, He = *Hymenoscyphus ericae*, 8 = *Hyaloscypha bicolor*, Hm = *Hebeloma mesophaeum*, Ar = *Amanita rubescens*, Tt = *Thelephora terrestris*, Lb = *Laccaria bicolor*.

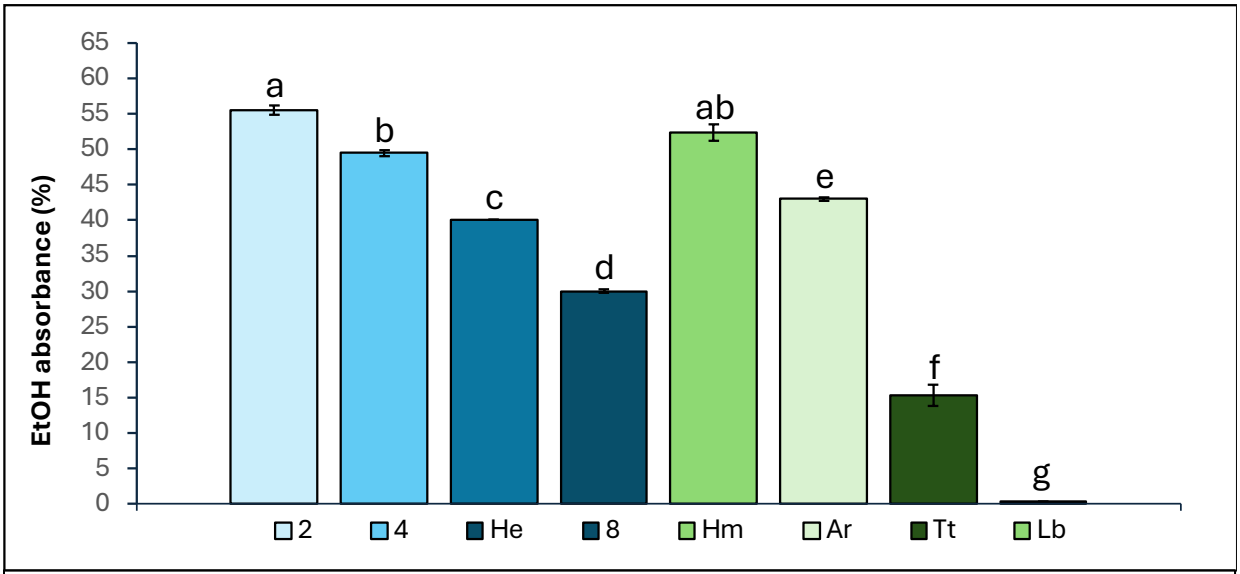

Fig. 4: Surface hydrophobicity (± SE) of four ERMF (blue), and four ECMF (green) measured using the ethanol percentage test on 9 spots per sample, with n = 5 for every species. Higher ethanol absorbance indicates higher surface hydrophobicity. Differences in hydrophobicity across fungal species are signified with different letters as indicated by a Wilcoxon rank sum test ($p<0,05$). 2 = *Oidiodendron maius*, 4 = *Oidiodendron maius*, He = *Hymenoscyphus ericae*, 8 = *Hyaloscypha bicolor*, Hm = *Hebeloma mesophaeum*, Ar = *Amanita rubescens*, Tt= *Thelephora terrestris*, Lb = *Laccaria bicolor*.

More specifically, localized peak heights for aromatic C–H stretching were generally higher in AMF and ERMF compared to ECMF (Fig. 6), with the notable exception of *O. maius (4)*, which exhibited the lowest value overall (Table 1). A similar trend was observed for aliphatic C–H stretching and aldehyde/ketone C=O stretching, where AMF, along with ERMF, except for *O. maius (4)*, showed the highest absorbance values. In contrast, amide C–O absorption was lowest in AMF, comparable to ERMF, but consistently lower than in ECMF. Exceptions included *H. bicolor*, which displayed the highest C-O absorbance values, and *T. terrestris*, the only ECMF species showing low amide C–O absorbance values. Furthermore, absorption for aromatic C=C bonds was relatively consistent across species, though *H. bicolor* again stood out with the highest C=C absorbance values, while *O. maius* (4) showed the lowest. Finally, polysaccharide C–O stretching absorbance was generally lowest in AMF and highest in ECMF. Among individual strains, MUCL 49408 = *R. aggregatus* had the lowest absorption, while *L. bicolor* showed the highest.

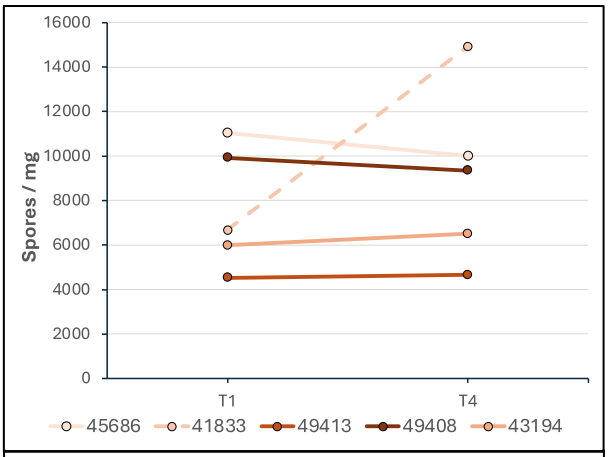

Fig. 5: Number of spores per mg of dry weight AMF necromass. Spores were counted at one (T1) and five weeks (T4) post decomposition. MUCL 45686 = *Glomus hoi*, MUCL 41833 = *Rhizophagus irregularis*, MUCL 49413 = *Rhizophagus intraradices*, MUCL 49408 = *Rhizophagus aggregatus*, MUCL 43194 = *Rhizophagus irregularis*.

Table 1: Summary of localized ATR-FTIR peak heights of undecomposed mycorrhizal fungal necromass. Differences in absorbance between the different fungal species at selected peaks were analysed using one-way ANOVA, followed by Tukey's HSD test. Darker colours indicate higher localized peak values. Different letters indicate statistically significant differences ($P \leq 0.05$). MUCL 45686 = *Glomus hoi*, MUCL 41833 = *Rhizophagus irregularis*, MUCL 49413 = *Rhizophagus intraradices*, MUCL 49408 = *Rhizophagus aggregatus*, MUCL 43194 = *Rhizophagus irregularis,* 2 = *Oidiodendron maius*, 4 = *Oidiodendron maius*, He = *Hymenoscyphus ericae*, 8 = *Hyaloscypha bicolor*, Hm = *Hebeloma mesophaeum*, Ar = *Amanita rubescens*, Tt= *Thelephora terrestris*, Lb = *Laccaria bicolor*.

	Localized peak height																					
Functional group	49408		49413		43194		41833		45686		8		He		4		Tt		Lb		Hm		Ar	
Aromatic C-H	0,014	bcd	0,019	b	0,018	b	0,014	bcd	0,016	bc	0,041	a	0,014	bcd	0,008	cd	0,006	cd	0,005	d	0,005	d	0,005	d
Aliphatic C-H	0,142	ab	0,173	a	0,187	a	0,189	a	0,181	a	0,145	ab	0,189	a	0,085	bc	0,059	c	0,048	c	0,030	c	0,022	c
Aldehydes-ketones C=O	0,200	ab	0,226	a	0,263	a	0,258	a	0,228	a	0,158	ab	0,255	a	0,108	bc	0,030	c	0,040	c	0,028	c	0,020	c
Amide C=O	0,034	e	0,038	e	0,035	e	0,038	e	0,036	e	0,099	a	0,055	bcde	0,049	cde	0,044	de	0,088	ab	0,078	abcd	0,079	abc
Aromatic C=C	0,036	bcd	0,053	abc	0,036	bc	0,062	abc	0,062	abc	0,076	a	0,035	bc	0,028	c	0,042	abc	0,058	abc	0,055	abc	0,066	ab
Polysacharide C-O	0,048	d	0,078	abcd	0,059	bcd	0,061	bcd	0,067	abcd	0,082	abcd	0,062	abcd	0,054	cd	0,105	ab	0,107	a	0,094	abc	0,086	abcd

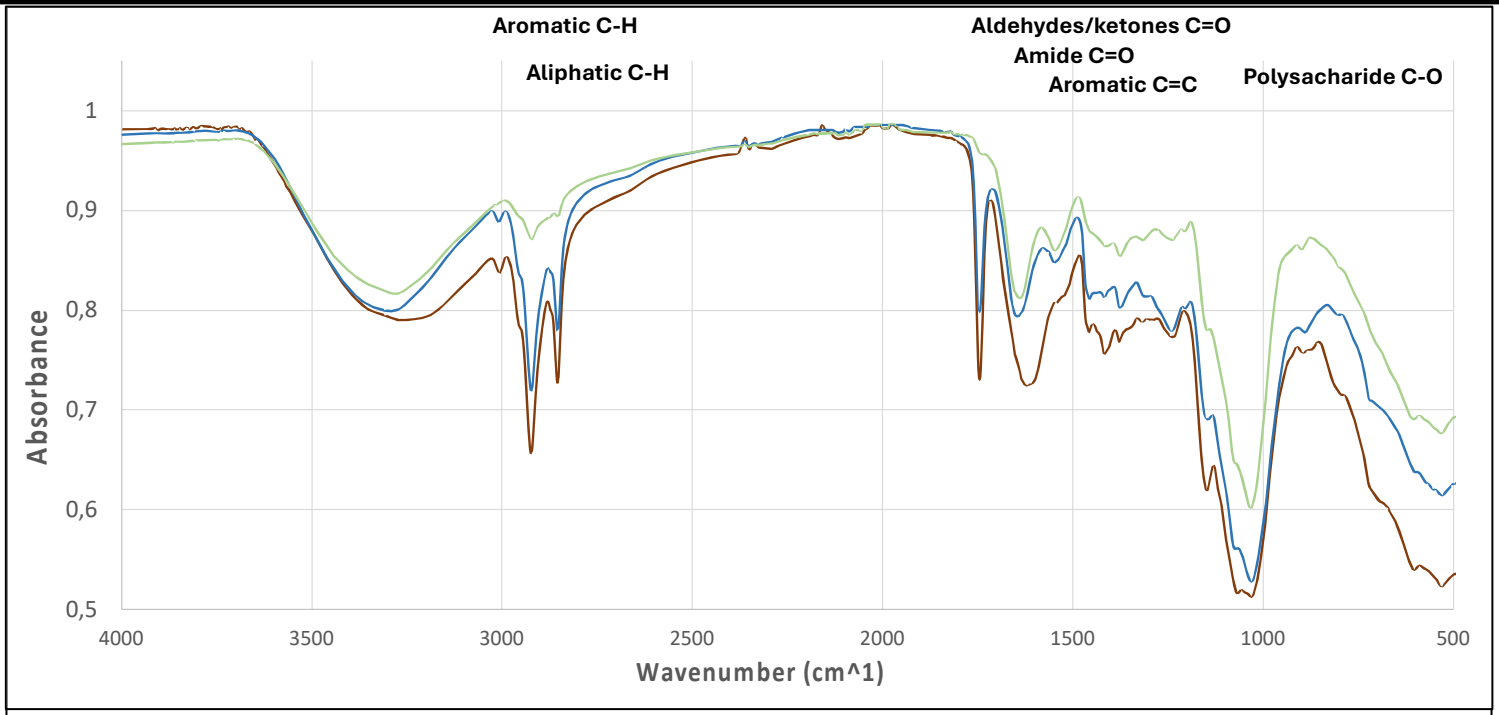

Fig. 6: ATR-FTIR spectra of undecomposed mycorrhizal fungal necromass. Spectra shown in this figure include guild averages of AMF (red), ERMF (blue) and ECMF (green).

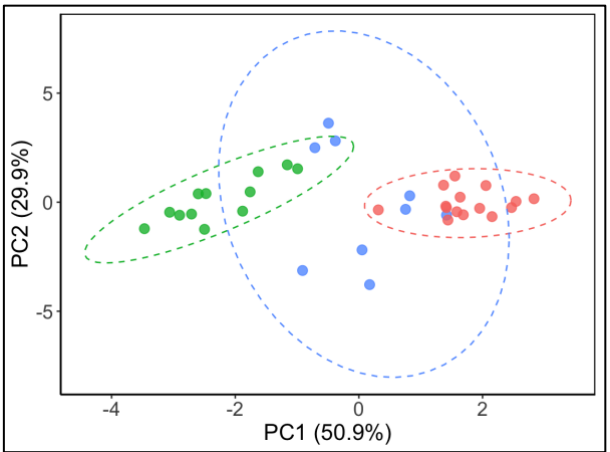

Fig. 7: Principal component analysis biplot for localized FTIR peak heights of undecomposed AMF necromass (red), ERMF necromass (blue), and ECMF

DISCUSSION

This is the first study to report and compare the decomposition of AMF, ERMF, and ECMF, showing the first results on AMF decomposition. The decomposition rates of AMF were considerably lower compared to ERMF and ECMF (Fig. 1). At week five, the relative mass remaining of AMF was approximately twice that of the ERMF and ECMF guild averages at week three (Fig. S1). Furthermore, there were significant intra-guild differences in necromass loss at three weeks of decomposition, especially within ERMF and ECMF (Fig. 2).

Firstly, differences in decomposition rates were expected to result from differences in melanin content, which has been reported as a key predictor of mycorrhizal recalcitrance due to its complex aromatic structure that resists microbial decomposition (50), and its ability to inhibit degrading enzymes (32). Additionally, based on their shared evolutionary history, resulting in similar functional traits and environmental distributions, we hypothesized that melanin levels would be consistent among species within each mycorrhizal guild. Specifically, ERMF, typically found in dry heathland ecosystems, were expected to exhibit higher melanin levels. However, this pattern was not observed, with melanin levels being comparable across species, apart from *H. ericae* which showed the highest melanin content of all examined species (Fig. 3). Moreover, *H. ericae* did not exhibit the highest recalcitrance (Fig. 2). Instead, its decomposition rate was comparable to that of *H. bicolor*, which had a high, though significantly lower melanin content. Unexpectedly, *T. terrestris* and *L. bicolor* also showed similar recalcitrance levels to both *H. ericae* and *H. bicolor*, despite having the lowest melanin concentrations (Fig. 3). Furthermore, AMF, despite being the most recalcitrant group overall, had melanin levels similar to those of *A. rubescens* and *H. mesophaeum*, which were the least recalcitrant.

Considering these observations, melanin did not serve as a reliable predictor for recalcitrance in our study. One possible explanation is that overall melanin concentrations were relatively low. *H. ericae* exhibited the highest levels, with an average concentration of approximately 43 mg/g. This is low compared to other studies, where melanin concentrations of over 200 mg/g have been reported (44, 51, 52). In this way, the differences in melanin content we observed were not as pronounced and may have been insufficient to drive the slower decomposition rates previously associated with higher melanin levels. The low melanin content observed in our study may be attributed to melanisation being a plastic trait that is typically induced under stressful conditions (53). In this way, a single fungal species can exhibit markedly different melanin levels depending on the environmental stressors it encounters (51). Likewise, the culturing conditions used in this study, namely nutrient-rich and well-hydrated media without external stressors, likely contributed to the low melanin levels observed.
Furthermore, the inconsistent relationship between melanin content and decomposition rates reported in this and at least one other study (44) may be partly explained by the variation in melanin types synthesized by different fungal species (54). Melanin refers to a group of heterogeneous molecules, classified based on the chemical structure and composition of their monomer subunits. Depending on the fungal species and environmental triggers, different types of melanin can be produced (54, 55). Ascomycetes, i.e., the ERMF in our study, are more prevalently associated with allomelanins, which are N-free forms of melanin (56). Contrastingly, Basidiomycetes, i.e., the ECMF in this study, are more commonly associated with pheomelanins, which contain N in

the form of cysteine (57). This may render pheomelanins a more interesting nutrient source for decomposers, reducing the recalcitrance of ECMF necromass. Moreover, different types of melanin can manifest differently across fungal species, being strongly embedded in the chitin-based cell walls or loosely associated in granular patches on the outer surface of the cell (58-60). Taken together, melanin may not consistently indicate fungal recalcitrance as previously reported, depending on the fungal species and environmental conditions.

Apart from melanisation, we hypothesized that mycorrhizal species with more hydrophobic mycelia would exhibit slower decomposition rates due to the formation of hydrophobic aggregates, which are less accessible to decomposers and more difficult to transport across intracellular spaces (35). However, no association between higher hydrophobicity (Fig. 4) and decomposition rates was observed. This confirms previous findings that, unlike plant litter, fungal hydrophobicity is not a strong predictor for decomposition rates (44). In contrast, a slight positive trend was observed, with species exhibiting higher surface hydrophobicity levels tending to decompose more slowly. This pattern may be caused by the ability of decomposer microorganisms to produce surfactants to access hydrophobic substrates, thereby creating an environment favourable for hydrophobic decomposition (61).

Additionally, we considered AMF spores to be a potential contributor to their recalcitrance. Unlike the ERMF and ECMF species, the culturing conditions for AMF permitted the inclusion of spores, which constituted a substantial portion of their necromass. Given that spores are reproductive structures known for their resistance to decay, we hypothesized that spore presence could be a significant predictor of recalcitrance in AMF (62). For these reasons, we quantified the number of spores per mg of dry weight of necromass at one week and four weeks post-decomposition. Spores were expected to be more recalcitrant than hyphae, showing a relative increase in abundance per milligram of dry weight over time. Our results did not support this hypothesis (Fig. 5), with only MUCL 41833 = *R. irregularis* showing a distinct increase in spore content. This suggests that the decomposition of spores and hyphae might be a more gradual process, with spores decomposing more slowly than hyphae on a level that was not observable through our method, which assessed spore persistence by manually counting the number of intact spores in a necromass sample. However, this was only observed in strain 41833, so no general conclusions can be made.

FTIR spectra of AMF were generally more similar to ERMF than to ECMF (Fig. 7). This was evident in their higher values for aromatic C–H stretching, aliphatic C–H stretching, and aldehyde/ketone C=O stretching compared to ECMF (Fig. 6). Our study aligns with previous research in showing that fungal species with higher absorbance values for aromatic constituents have lower decomposition rates (30). Interestingly, values linked to aromatic C=C bonds, in contrast to aromatic C-H bonds, did not entirely follow this trend, showing more similar absorbance values across all species (Table 1), which could be caused by different fungal species producing different kinds of melanin (63, 64). Additionally, AMF showed higher aliphatic C–H absorption values, which were not reflected in their decomposition rates, as they are typically associated with lipids that degrade rapidly (30). However, the increased aliphatic content is likely caused by the increased lipid content inside their spores, which serve as an energy source for spore germination (65). Likewise, the mass loss expected from higher aliphatic content could be inhibited by the fact that they are protected by thick spore walls (66). Moreover, AMF showed lower absorption values in both the amide C=O and polysaccharide C–O stretching regions compared to ERMF and ECMF species. This could help explain the low mass loss AMF, as polysaccharides and proteins are typically the first to decompose after incubation (25). Finally, the spectra of *T. terrestris* and *L. bicolor* were much more similar to the other rapidly decomposing ECMF species, i.e., *H. mesophaeum* and *A. rubescens*, despite showing similar recalcitrance to *H. bicolor* after three weeks of decomposition (Fig. 2). In particular, the FTIR spectrum of *T. terrestris* raises questions, as its high polysaccharide and low aromatic compound levels did not correspond with its comparatively high recalcitrance. This discrepancy underscores the need to look beyond the commonly studied biochemical traits in relation to fungal decomposition. The fact that certain fungal biomass

characteristics, such as melanin, have been widely recognized as key contributors to mycorrhizal necromass recalcitrance (67, 68) should not overshadow the potential role of other, understudied molecules that could influence decomposition rates.

Likewise, we suggest that future studies analyze the entire FTIR spectrum in relation to mycorrhizal decomposition rates and track these changes throughout the decomposition process. Additionally, melanin characterization should be conducted to identify the specific types of melanin present and their localization within fungal tissues, helping to determine which melanin forms most significantly contribute to necromass recalcitrance across fungal groups. Furthermore, separate biochemical analyses of AMF spores and hyphae are needed to assess whether spore recalcitrance contributes to the overall persistence of AMF necromass, potentially explaining the subtle spectral differences between AMF and ERMF (Fig. 7) and their divergent decomposition rates.

CONCLUSION

This study provides essential information towards accurate representation of mycorrhizal fungal necromass turnover in global carbon models, reporting the first ever results on AMF decomposition and showing them to be distinctly recalcitrant relative to ERMF and ECMF, highlighting their potential role as a stable soil carbon storage pool. Importantly, we found that melanin and hydrophobicity were not consistent predictors of decomposition rates, demonstrating that commonly described recalcitrance characteristics do not fully explain necromass decomposition patterns. These results not only expand fundamental knowledge of fungal necromass turnover but also carry broader implications for modelling soil carbon dynamics in terrestrial ecosystems.

REFERENCES

1. Tarnocai C, Canadell JG, Schuur EAG, Kuhry P, Mazhitova G, Zimov S. Soil organic carbon pools in the northern circumpolar permafrost region. Global Biogeochemical Cycles. 2009;23(2).
2. Hawkins H-J, Cargill RIM, Van Nuland ME, Hagen SC, Field KJ, Sheldrake M, et al. Mycorrhizal mycelium as a global carbon pool. Current Biology. 2023;33(11):R560-R73.
3. Petraglia A, Cacciatori C, Chelli S, Fenu G, Calderisi G, Gargano D, et al. Litter decomposition: effects of temperature driven by soil moisture and vegetation type. Plant and Soil. 2019;435:187-200.
4. Zhang W, Gao D, Chen Z, Li H, Deng J, Qiao W, et al. Substrate quality and soil environmental conditions predict litter decomposition and drive soil nutrient dynamics following afforestation on the Loess Plateau of China. Geoderma. 2018;325:152-61.
5. Canessa R, van den Brink L, Saldaña A, Rios RS, Hättenschwiler S, Mueller CW, et al. Relative effects of climate and litter traits on decomposition change with time, climate and trait variability. Journal of Ecology. 2021;109(1):447-58.
6. Sierra CA, Malghani S, Loescher HW. Interactions among temperature, moisture, and oxygen concentrations in controlling decomposition rates in a boreal forest soil. Biogeosciences. 2017;14(3):703-10.
7. Shi Z, Allison SD, He Y, Levine PA, Hoyt AM, Beem-Miller J, et al. The age distribution of global soil carbon inferred from radiocarbon measurements. Nature Geoscience. 2020;13(8):555-9.
8. Soudzilovskaia NA, van Bodegom PM, Terrer C, Zelfde Mvt, McCallum I, Luke McCormack M, et al. Global mycorrhizal plant distribution linked to terrestrial carbon stocks. Nature Communications. 2019;10(1):5077.

9. Pandey D, Kehri HK, Zoomi I, Akhtar O, Singh AK. Mycorrhizal fungi: Biodiversity, ecological significance, and industrial applications. Recent Advancement in White Biotechnology Through Fungi: Volume 1: Diversity and Enzymes Perspectives. 2019:181-99.
10. Smith SE, Read DJ. Mycorrhizal symbiosis: Academic press; 2010.
11. Kakouridis A, Hagen JA, Kan MP, Mambelli S, Feldman LJ, Herman DJ, et al. Routes to roots: direct evidence of water transport by arbuscular mycorrhizal fungi to host plants. New Phytologist. 2022;236(1):210-21.
12. Brundrett M. Mycorrhizal associations and other means of nutrition of vascular plants: Understanding the global diversity of host plants by resolving conflicting information and developing reliable means of diagnosis. Plant and Soil. 2009;320:37-77.
13. Heklau H, Schindler N, Buscot F, Eisenhauer N, Ferlian O, Prada Salcedo LD, et al. Mixing tree species associated with arbuscular or ectotrophic mycorrhizae reveals dual mycorrhization and interactive effects on the fungal partners. Ecol Evol. 2021;11(10):5424-40.
14. Brundrett MC, Tedersoo L. Evolutionary history of mycorrhizal symbioses and global host plant diversity. New Phytologist. 2018;220(4):1108-15.
15. Tedersoo L, Bahram M, Põlme S, Kõljalg U, Yorou NS, Wijesundera R, et al. Global diversity and geography of soil fungi. science. 2014;346(6213):1256688.
16. Andrino A, Guggenberger G, Sauheitl L, Burkart S, Boy J. Carbon investment into mobilization of mineral and organic phosphorus by arbuscular mycorrhiza. Biology and Fertility of Soils. 2021;57(1):47-64.
17. Thirkell TJ, Cameron DD, Hodge A. Resolving the 'nitrogen paradox'of arbuscular mycorrhizas: fertilization with organic matter brings considerable benefits for plant nutrition and growth. Plant, Cell & Environment. 2016;39(8):1683-90.
18. Staddon PL, Ramsey CB, Ostle N, Ineson P, Fitter AH. Rapid turnover of hyphae of mycorrhizal fungi determined by AMS microanalysis of 14C. Science. 2003;300(5622):1138-40.
19. Cheeke TE, Phillips RP, Kuhn A, Rosling A, Fransson P. Variation in hyphal production rather than turnover regulates standing fungal biomass in temperate hardwood forests. Ecology. 2021;102(3):e03260.
20. Guo W, Ding J, Wang Q, Yin M, Zhu X, Liu Q, et al. Soil fertility controls ectomycorrhizal mycelial traits in alpine forests receiving nitrogen deposition. Soil Biology and Biochemistry. 2021;161:108386.
21. Clark Rá, Zeto S. Mineral acquisition by arbuscular mycorrhizal plants. Journal of plant Nutrition. 2000;23(7):867-902.
22. Beidler KV, Phillips RP, Andrews E, Maillard F, Mushinski RM, Kennedy PG. Substrate quality drives fungal necromass decay and decomposer community structure under contrasting vegetation types. Journal of Ecology. 2020;108(5):1845-59.
23. Schaffer-Morrison SAZ, Zak DR. Mycorrhizal fungal and tree root functional traits: Strategies for integration and future directions. Ecosphere. 2023;14(2):e4437.
24. Huang W, van Bodegom PM, Declerck S, Heinonsalo J, Cosme M, Viskari T, et al. Mycelium chemistry differs markedly between ectomycorrhizal and arbuscular mycorrhizal fungi. Communications Biology. 2022;5(1):398.
25. Ryan ME, Schreiner KM, Swenson JT, Gagne J, Kennedy PG. Rapid changes in the chemical composition of degrading ectomycorrhizal fungal necromass. Fungal Ecology. 2020;45:100922.

26. Drigo B, Anderson IC, Kannangara GSK, Cairney JWG, Johnson D. Rapid incorporation of carbon from ectomycorrhizal mycelial necromass into soil fungal communities. Soil Biology and Biochemistry. 2012;49:4-10.
27. Singaravelan N, Grishkan I, Beharav A, Wakamatsu K, Ito S, Nevo E. Adaptive melanin response of the soil fungus Aspergillus niger to UV radiation stress at "Evolution Canyon", Mount Carmel, Israel. PloS one. 2008;3(8):e2993.
28. Fernandez CW, Koide RT. The function of melanin in the ectomycorrhizal fungus Cenococcum geophilum under water stress. Fungal Ecology. 2013;6(6):479-86.
29. Nosanchuk JD, Casadevall A. The contribution of melanin to microbial pathogenesis. Cellular microbiology. 2003;5(4):203-23.
30. Fernandez CW, Heckman K, Kolka R, Kennedy PG. Melanin mitigates the accelerated decay of mycorrhizal necromass with peatland warming. Ecol Lett. 2019;22(3):498-505.
31. Kuo M-J, Alexander M. Inhibition of the lysis of fungi by melanins. Journal of Bacteriology. 1967;94(3):624-9.
32. Bull A. Inhibition of Polysaccharases in Relation by Melanin: to Mycolysis Enzyme Inhibition A role for melanin in the resistance of fungi to microbial lysis is evident from recent reports. The present investigation was dire. Archives of Biochemistry and Biophysics. 1970:345-56.
33. Maillard F, Michaud TJ, See CR, DeLancey LC, Blazewicz SJ, Kimbrel JA, et al. Melanization slows the rapid movement of fungal necromass carbon and nitrogen into both bacterial and fungal decomposer communities and soils. mSystems. 2023;8(4):e0039023.
34. Feofilova EP, Ivashechkin AA, Alekhin AI, Sergeeva YE. Fungal spores: Dormancy, germination, chemical composition, and role in biotechnology (review). Applied Biochemistry and Microbiology. 2012;48(1):1-11.
35. Song XY, Spaccini R, Pan G, Piccolo A. Stabilization by hydrophobic protection as a molecular mechanism for organic carbon sequestration in maize-amended rice paddy soils. Science of The Total Environment. 2013;458-460:319-30.
36. Goebel M-O, Bachmann J, Woche SK, Fischer WR. Soil wettability, aggregate stability, and the decomposition of soil organic matter. Geoderma. 2005;128(1):80-93.
37. Steinberg P, Rillig M. Differential decomposition of arbuscular mycorrhizal fungal hypha and glomalin. Soil Biology & Biochemistry - SOIL BIOL BIOCHEM. 2003;35:191-4.
38. Lugones L, Jong J, Vries O, Jalving R, Dijksterhuis J, Wösten H. The SC15 protein of Schizophyllum commune mediates formation of aerial hyphae and attachment in the absence of the SC3 hydrophobin. Molecular microbiology. 2004;53:707-16.
39. Samuel Obeng A, Dunne J, Giltrap M, Tian F. Soil organic matter carbon chemistry signatures, hydrophobicity and humification index following land use change in temperate peat soils. Heliyon. 2023;9(9):e19347.
40. G. Muller GFV, Jena,. Malt extract agar. Bodembiologie
. 1965:230.
41. Collins CH. CDOX agar. Microbiological Methods, London. 1967.
42. Declerck S, Strullu, D.G., Plenchette, C. Monoxenic culture of the intraradical forms of Glomus sp. isolated from a tropical ecosystem: a proposed methodology for germplasm collection. Mycologia. 1998. ;90:6.
43. Chau HW, Goh YK, Si BC, Vujanovic V. Assessment of alcohol percentage test for fungal surface hydrophobicity measurement. Lett Appl Microbiol. 2010;50(3):295-300.

44. Lenaers M, Reyns W, Czech J, Carleer R, Basak I, Deferme W, et al. Links Between Heathland Fungal Biomass Mineralization, Melanization, and Hydrophobicity. Microbial Ecology. 2018;76(3):762-70.
45. Nouwen O RF, Kohout P, Baldrian P, Eisenhauer N, Beenaerts N,. Towards understanding the impact of mycorrhizal fungal environments on the functioning of terrestrial ecosystems [Preprint]. 2023.
46. van de Voorde TFJ, van der Putten WH, Bezemer TM. Soil inoculation method determines the strength of plant–soil interactions. Soil Biology and Biochemistry. 2012;55:1-6.
47. Liu Z, Zhang C, Ma J, Peng Q, Du X, Sun Se, et al. Extraction Methods Determine the Quality of Soil Microbiota Acquisition. Microorganisms. 2024;12(2):403.
48. Wallander H, Göransson H, Rosengren U. Production, standing biomass and natural abundance of 15N and 13C in ectomycorrhizal mycelia collected at different soil depths in two forest types. Oecologia. 2004;139(1):89-97.
49. Zhai J, Cong L, Yan G, Wu Y, Liu J, Wang Y, et al. Influence of fungi and bag mesh size on litter decomposition and water quality. Environmental Science and Pollution Research. 2019;26(18):18304-15.
50. Butler M, Day A. Destruction of fungal melanins by ligninases of Phanerochaete chrysosporium and other white rot fungi. International Journal of Plant Sciences. 1998;159(6):989-95.
51. Fernandez CW, Kennedy PG. Melanization of mycorrhizal fungal necromass structures microbial decomposer communities. Journal of Ecology. 2018;106(2):468-79.
52. Fernandez C, Koide RT. Initial melanin and nitrogen concentrations control the decomposition of ectomycorrhizal fungal litter. Soil Biology and Biochemistry. 2014;77:150–7.
53. Chambergo FS, Valencia EY. Fungal biodiversity to biotechnology. Applied microbiology and biotechnology. 2016;100:2567-77.
54. Suthar M, Dufossé L, Singh SK. The Enigmatic World of Fungal Melanin: A Comprehensive Review. J Fungi (Basel). 2023;9(9).
55. Eisenman HC, Casadevall A. Synthesis and assembly of fungal melanin. Applied microbiology and biotechnology. 2012;93:931-40.
56. Ma X-P, Sun X-X. Melanin: biosynthesis, functions and health effects: Nova Science Publishers, Incorporated; 2012.
57. Ozeki H, Ito S, Wakamatsu K, Ishiguro I. Chemical characterization of pheomelanogenesis starting from dihydroxyphenylalanine or tyrosine and cysteine.: Effects of tyrosinase and cysteine concentrations and reaction time. Biochimica et Biophysica Acta (BBA)-General Subjects. 1997;1336(3):539-48.
58. Plonka PM, Grabacka M. Melanin synthesis in microorganisms--biotechnological and medical aspects. Acta biochimica polonica. 2006;53(3):429-43.
59. Leiman PG, Taylor NM. Reference module in life sciences. Elsevier; 2019.
60. Walker CA, Gómez BL, Mora-Montes HM, Mackenzie KS, Munro CA, Brown AJ, et al. Melanin externalization in Candida albicans depends on cell wall chitin structures. Eukaryotic cell. 2010;9(9):1329-42.
61. Ron EZ, Rosenberg E. Natural roles of biosurfactants. Environ Microbiol. 2001;3(4):229-36.
62. Deveautour C, Chieppa J, Nielsen UN, Boer MM, Mitchell C, Horn S, et al. Biogeography of arbuscular mycorrhizal fungal spore traits along an aridity gradient, and responses to experimental rainfall manipulation. Fungal Ecology. 2020;46:100899.

63. Sun S, Zhang X, Sun S, Zhang L, Shan S, Zhu H. Production of natural melanin by Auricularia auricula and study on its molecular structure. Food Chemistry. 2016;190:801-7.
64. Sansinenea E, Ortiz A. Melanin: a photoprotection for Bacillus thuringiensis based biopesticides. Biotechnology Letters. 2015;37(3):483-90.
65. Kameoka H, Gutjahr C. Functions of Lipids in Development and Reproduction of Arbuscular Mycorrhizal Fungi. Plant Cell Physiol. 2022;63(10):1356-65.
66. Bonfante-Fasolo P, Vian B. Wall texture in the spore of a vesicular-arbuscular mycorrhizal fungus. Protoplasma. 1984;120(1):51-60.
67. Fernandez CW, Koide RT. Initial melanin and nitrogen concentrations control the decomposition of ectomycorrhizal fungal litter. Soil Biology and Biochemistry. 2014;77:150-7.
68. Koide RT, Malcolm G. N concentration controls decomposition rates of different strains of ectomycorrhizal fungi. Fungal Ecology. 2009;2:197-202.

Acknowledgements – BA gratefully thanks the CMK microbiology group for giving him the opportunity to complete this senior internship. Furthermore, ON is thanked for his critical insights and guidance during this internship. Francois Rineau is thanked for his guidance during FTIR analysis. Jeff Vermeuelen is thanked for his help in the culturing of the fungal species.

Author contributions – NS, ON and BA conceived and designed the research. ON and BA performed experiments. BA performed data analysis. ON and BA carefully edited the manuscript.

Supplemental figures: Mycorrhizal necromass decomposition

Table S1: Initial mass of samples used in the decomposition experiment for one week (T1), two weeks (T2), and three weeks (T3). MUCL 45686 = *Glomus hoi*, MUCL 41833 = *Rhizophagus irregularis*, MUCL 49413 = *Rhizophagus intraradices*, MUCL 49408 = *Rhizophagus aggregatus*, MUCL 43194 = *Rhizophagus irregularis*, 2 = *Oidiodendron maius*, 4 = *Oidiodendron maius*, He = *Hymenoscyphus ericae*, 8 = *Hyaloscypha bicolor*, Hm = *Hebeloma mesphaeum*, Ar = *Amanita rubescens*, Tt = *Thelephora terrestris*, Lb = *Laccaria bicolor*.

		Initial mass (mg)		
Guild	Species	T1	T2	T3
AMF	45686	12,1	12,3	12,1
AMF	41833	10,6	10,9	11
AMF	49413	16,4	16,2	16,8
AMF	43194	10,7	10,5	10,4
AMF	43194	10,4	10,2	13,1
AMF	49408	16,9	16,5	16,7
AMF	49408	17,3	16,5	16,6
AMF	49408	16,5	16,4	16,5
ERM	He	110,1	114,8	109,8
ERM	He	112,3	112,3	105,9
ERM	He	126,9	107,2	110,9
ERM	He	101,78	110,5	99,3
ERM	He	106,83	93,8	106,6
ERM	2	59,2	60,1	59,9
ERM	2	62,3	59,4	70,9
ERM	2	59,4	60	70,5
ERM	2	60	59,4	60
ERM	2	69,2	59,6	59,7
ERM	4	90	72,2	79
ERM	4	77,8	60,9	92,4
ERM	4	70,4	80	70,7
ERM	4	51,8	65,3	77
ERM	4	70	70,4	84,7
ERM	8	118	90	109,6
ERM	8	103	109,5	108,3
ERM	8	103,7	109,8	110,5
ERM	8	110,8	114,3	110,2
ERM	8	110,6	108	110
ECM	Ar	109,8	110,6	110,2
ECM	Ar	110,6	110	110
ECM	Ar	102,8	111,1	104,3
ECM	Ar	109	111	106,5
ECM	Ar	108,1	108,3	109,5
ECM	Hm	68,7	69,8	70
ECM	Hm	70,1	69,2	67,9
ECM	Hm	71,5	65,4	69,1
ECM	Hm	69,5	67,6	66,9
ECM	Hm	68,5	65,8	69,7
ECM	Tt	106,9	109,8	111
ECM	Tt	111,2	117,2	112
ECM	Tt	112,6	110,4	112
ECM	Tt	108,8	109,2	110,6
ECM	Tt	110,4	110,2	110,6
ECM	Lb	110,4	105,6	110,4
ECM	Lb	110,1	110,7	109,3
ECM	Lb	108,2	109,8	110,5
ECM	Lb	110,1	110	107,8
ECM	Lb	115,5	109,2	109,6

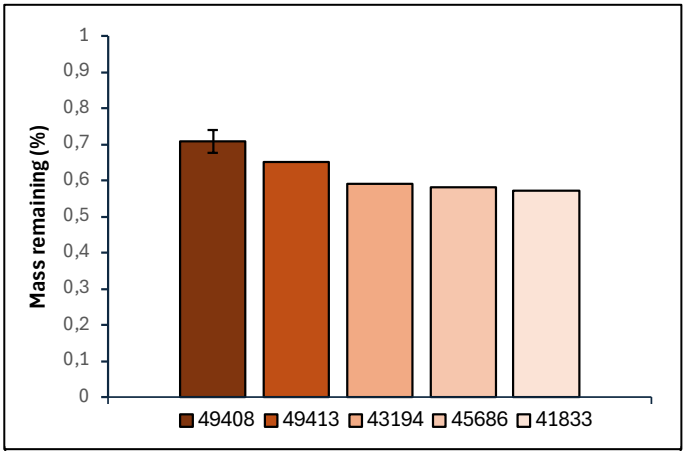

Fig. S1: Relative mass remaining of five AMF species at five weeks post-decomposition using a controlled pot decomposition experiment. The mass remaining is specified as the percentage of dry weight remaining compared to the original non-decomposed necromass sample. MUCL 45686 = *Glomus hoi* (n=1), MUCL 41833 = *Rhizophagus irregularis* (n=1), MUCL 49413 = *Rhizophagus intraradices* (n=1), MUCL 49408 = *Rhizophagus aggregatus* (n=3), MUCL 43194 = *Rhizophagus irregularis* (n=1)